Supplemental Document for "Rendering Iridescent Rock Dove Neck Feathers"

Weizhen Huang
University of Bonn
Bonn, Germany
whuang@cs.uni-bonn.de

Sebastian Merzbach
University of Bonn
Bonn, Germany
merzbach@cs.uni-bonn.de

Clara Callenberg
University of Bonn
Bonn, Germany
callenbe@cs.uni-bonn.de

Doekele G. Stavenga
University of Groningen
Groningen, Netherlands
d.g.stavenga@rug.nl

Matthias B. Hullin
University of Bonn
Germany
hullin@cs.uni-bonn.de

1 THIN FILM INTERFERENCE

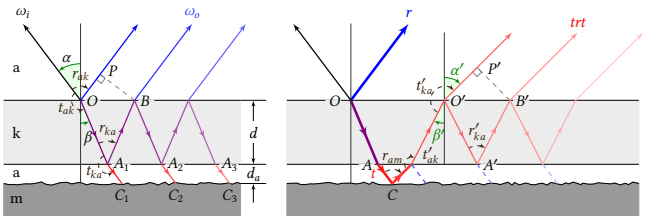

Figure 1: Thin-film interference. Left: thin-film reflection (blue arrows). Right: thin-film reflection (blue) and the background component (red), which is transmitted through the keratin layer, reflected on the melanin layer, then transmitted back through the keratin layer.

Airy Formula [Yeh 2005]. The optical path difference (OPD) for thin-film reflection and transmission is $\mathcal{D} = \eta_k(\overline{OA_1} + \overline{A_1B}) - \eta_a\overline{OP} = 2d\eta_k \cos\beta$ (Fig. 1). Thus, the complex thin-film reflection coefficient r is computed as

$$\begin{aligned} r &= r_{ak} + t_{ak}r_{ka}t_{ka}e^{i\Delta\psi_r} + t_{ak}r_{ka}r_{ka}^2t_{ka}e^{2i\Delta\psi_r} + \dots \\ &= r_{ak} + \sum_{n=0}^{+\infty} t_{ak}r_{ka}t_{ka}e^{i\Delta\psi_r}\left[r_{ka}^2e^{i\Delta\psi_r}\right]^n \\ &= r_{ak} + \frac{t_{ak}r_{ka}t_{ka}e^{i\Delta\psi}}{1 - r_{ka}^2e^{i\Delta\psi}}, \end{aligned} \tag{1}$$

and the complex thin-film transmission coefficient

$$\begin{aligned} t &= t_{ak}t_{ka} + t_{ak}r_{ka}^2t_{ka}e^{i\Delta\psi} + t_{ak}r_{ka}^4t_{ka}e^{2i\Delta\psi} + \dots \\ &= \sum_{n=0}^{+\infty} t_{ak}t_{ka}\left[r_{ka}^2e^{i\Delta\psi}\right]^n \\ &= \frac{t_{ak}t_{ka}}{1 - r_{ka}^2e^{i\Delta\psi}}. \end{aligned} \tag{2}$$

The OPD for the TRT component is similarly computed as $\mathcal{D}' = \eta_k(\overline{OA'} + \overline{A'B}) - \eta_a\overline{O'P'} = 2d\eta_k \cos\beta'$. Thus,

$$\begin{aligned} I_{\mathrm{TRT}} &= \left| tr_{am}t'_{ak}t'_{ka} + tr_{am}t'_{ak}\left(r'_{ka}\right)^2 t'_{ka}e^{i\Delta\psi'} + \dots \right|^2 \\ &= \left| \frac{tr_{am}t'_{ak}t'_{ka}}{1 - \left(r'_{ka}\right)^2 e^{i\Delta\psi'}} \right|^2. \end{aligned} \tag{3}$$

Thin-film interference with curvature. We perform a 2D analysis of curved thin film interference. Fig. 2a shows parallel light hitting a hollow cylindrical tube. The two indicated incident rays with the same axis of symmetry interfere, as their outgoing directions are also parallel. The optical path difference is the difference between the optical path length of the blue and red paths. Further orders of interference are computed analogously.

We compare the reflectance off such a cylindrical tube as a function of the difference between the incoming and outgoing directions, with $\lambda = 520\,\mathrm{nm}$, $d = 650\,\mathrm{nm}$. We choose a large curvature radius $r_l = 40\,\mu\mathrm{m}$ and a small curvature radius $r_s = 4\,\mu\mathrm{m}$, and compare the reflectance with a flat thin film. As shown in Fig. 2b, there is almost no difference between the reflectance off a flat and a curved keratin thin film, except at near-grazing angles, where total internal reflection happens, as on a convex curved thin film $\phi'_t > \phi_t$. These angles can generally not be observed due to the overlapping geometry of the barbules, and the curvature radius is only small at the edge of the barbule. Thus, we assume the barbule to be piecewise flat for simplicity.

2 MELANIN TRANSMITTANCE

In our model we consider thin-film interference of the keratin layer (R component), and the transmission through the keratin layer times the reflection off the melanin layer times thi transmission through the keratin layer back into the eyes (TRT component), plus the transmission through the barbule gaps (T component). As we have seen, the intensity of the TRT component is already very low, and all subsequent components are ignored because of melanin's large absorptance. The refractive index of melanin is $1.648 + 0.0632i$ at 589 nm [Stavenga et al. 2015], which means an absorption coefficient of $\alpha = \frac{0.0632 \times 4\pi}{589\,\mathrm{nm}} = 0.0013\,\mathrm{nm}^{-1}$. After traveling $2\,\mu\mathrm{m}$ of melanin granules, the light intensity would be attenuated by $\exp(-\alpha \times 2\,\mu\mathrm{m}) = 6.7\%$, which is fairly low. Melanin-rich dark

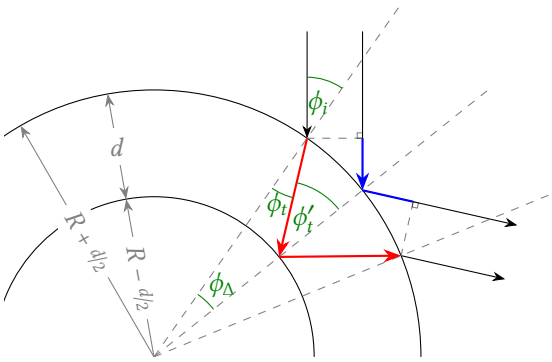

(a) Parallel rays hitting a cylindrical keratin tube

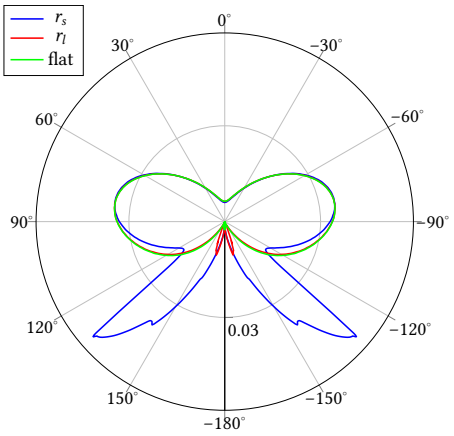

(b) Reflectance with piecewise flat assumption (green) plotted against analytically computed reflectance with curvature (blue and red). The red plot has a curvature radius of 40 µm, which is almost indistinguishable from the green plot. This is also the average curvature radius of a rock dove neck feather barbule. The blue plot has a curvature radius of 4 µm, showing a large difference at near-grazing angles. Such small radius only occurs at the edge of the barbule.

Figure 2: Illustration and reflectance plot of interference on a curved thin-film.

human hairs also have very low transmittance [Pharr 2016]. Unlike on human hairs, bird feathers overlap substantially so that backlit don't occur, thus, to be able to reach the eyes, further components must be reflected again on another feather underneath it, and possibly transmitted again through the feather, causing even more light to be absorbed. Such a contribution is very low.

3 ABLATION STUDY

3.1 Comparison to Circular Cross-Section

Models for rendering hair or fur usually assume a circular cross-section of the fibers. Fig. 3 shows a comparison of our model (left), which assumes an elliptical cross section of the barbules, to the BSDF produced by a circular cross section (right). Comparing to the scatterogram in Fig. 1c (top) of the main paper, our elliptical

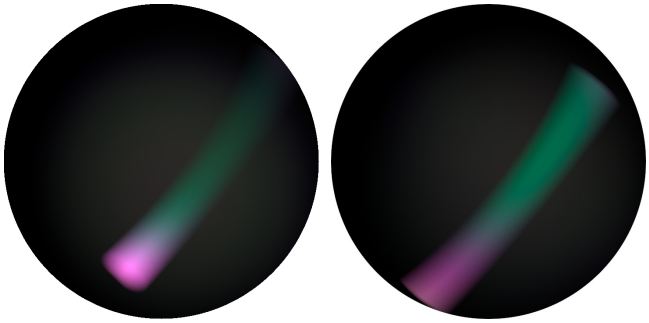

Figure 3: Left: Rendering of the barbule BSDF with an elliptical cross-section of the barbules ($b = 0.25$) as shown in Fig. 1c in the main paper. Right: Rendering of the barbule BSDF with a circular cross-section of the barbule ($b = 1$).

model is clearly much closer to the measurement than a circular model.

3.2 Other Parameters

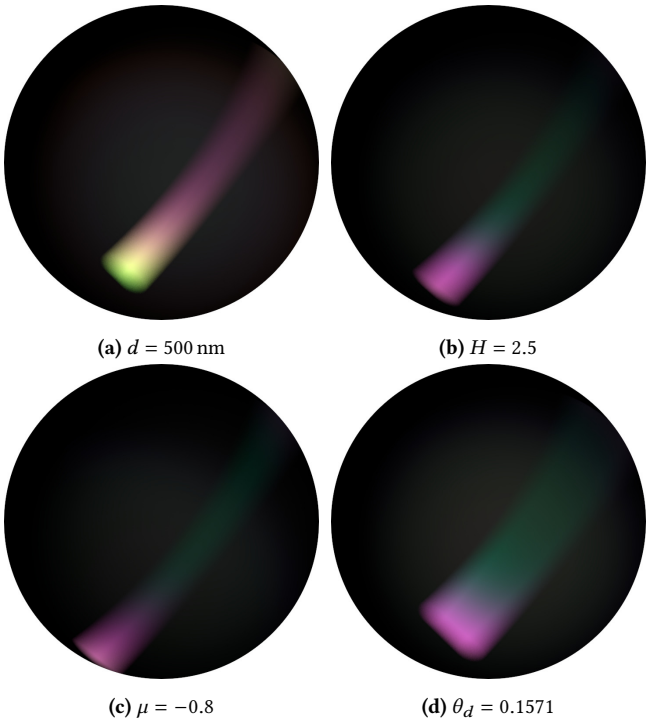

(a) $d = 500$ nm **(b)** $H = 2.5$

(c) $\mu = -0.8$ **(d)** $\theta_d = 0.1571$

Figure 4: Ablation study with parameters that differ from the one chosen in the main paper (compare to Fig. 3 (left)). One parameter is varied in each rendering: (a) keratin layer thickness changed from 590 nm to 500 nm, (b) barbule spacing changed from 1.25 to 2.5, (c) barbule orientation changed from -0.35 to -0.8, (d) circular arc opening angle changed from 0.0785 to 0.1571.

We also provide such an ablation study in Fig. 4 for other parameters in this model. As expected from Fig. 3 in the main paper, changing the thickness d of the keratin layer produces different scattered colors (Fig. 4a). Changing the spacing H and orientation μ of the barbules affects the visible normal distribution and the gap between the barbules, thus changing the intensity of the scattered light (Figs. 4b and 4c). With an increased spacing between the barbules and a larger inclination angle, the amount of transmitted light increases, so the intensity of the reflection is lowered. Increasing the opening angle θ_d of the barbule's circular arc in the longitudinal direction increases the scattering angle in the corresponding direction (Fig. 4d).

REFERENCES

Matt Pharr. 2016. The Implementation of a Hair Scattering Model. https://web.archive.org/web/20211205052753/https://www.pbrt.org/hair.pdf

Doekele G Stavenga, Hein L Leertouwer, Daniel C Osorio, and Bodo D Wilts. 2015. High refractive index of melanin in shiny occipital feathers of a bird of paradise. *Light: Science & Applications* 4, 1 (2015), e243–e243. https://doi.org/10.1038/lsa.2015.16

Pochi Yeh. 2005. *Optical waves in layered media.* Wiley.